

Upper rim site lipophilic calix[4]arenes as receptors for natural terpenes and functionally related solvent molecules: combined crystal structure and QMB sensor study†‡

Tobias Gruber,[§] Conrad Fischer,^a Wilhelm Seichter,^a Petra Bombicz^b and Edwin Weber^{*a}

Received 17th June 2010, Accepted 20th October 2010

DOI: 10.1039/c0ce00696c

Three upper rim site lipophilic calix[4]arenes **1–3** featuring different *para*-alkanoyl substituents at the phenolic moieties, *i.e.* *n*-hexanoyl, *n*-octanoyl and 3-cyclohexylpropanoyl groups, are reported to complex, aside from the common solvent molecule *n*-butanol, different keto and hydroxylic terpene guest molecules such as (–)-menthone, (–)-menthol or (+)-carvone in the solid state. Although for all six inclusion compounds described here, a strict 1 : 1 host : guest stoichiometry is observed, complementary size and polarity relationships between the cone shaped calixarene cavity and the guest molecule emerge from single crystal X-ray structural study. Dependent on the structure of the guest molecule, the calixarenes are arranged in a head-to-head or head-to-tail orientation in the crystalline packing, giving rise to capsular or otherwise deeply enclosed inclusion mode of the guest molecules, respectively. Furthermore, the *O*-acyl atoms of the calixarenes were found to be directly involved in host–guest interaction. In order to estimate the degree of isostructurality of the host frameworks and to examine the influence of the guest molecules on the solid-state conformation of these calixarene molecules, isostructurality comparison, cell similarity and molecular isometricity calculations were carried out revealing a rare case of supramolecular morphotropism for the pair of (–)-menthone and (–)-menthol inclusions of the *n*-hexanoyl substituted calixarene. Structure–inclusion property relationship was examined by QMB measurements of thin layers of the calixarenes. Vapor studies with different terpenes and common organic solvents show an increased affinity towards guest molecules with polar functionalities, whereas small solvent molecules like acetone are bound considerably better than the more bulky terpene molecules.

Introduction

After three productive decades, calixarenes continue to be a stimulating class of compounds with the calix[4]arene as the typical example.¹ One of its very attractive features is the cuplike structure provided by this molecule both in the solid state and in solution, from which this compound family derives the name and which is capable of hosting neutral guest molecules of complementary size. For the well-known conformationally fixed *p*-*tert*-butylcalix[4]arene the feature of gas-storage and diffusion in the crystalline state has been studied in detail^{2–4} and some of the resulting nonporous solids have been proven to form a well-defined stoichiometric 1 : 1 host–guest inclusion induced

by different guest species.⁵ Aside from the conformational mobility of the chalice the complexation behaviour seems to be determined by the nature of the substituents attached to the upper rim site.⁶ Thus, calix[4]arenes that carry lipophilic alkanoyl residues at the upper rim should prefer a cone conformation and are expected to form inclusion compounds with relatively large lipophilic molecules such as biologically interesting terpenes. However, so far this has been proven by X-ray structural analysis only in a single case where a hexanoyl substituted calix[4]arene and (+)-carvone were used.⁷ On the other hand, correspondingly modified alkanoyl calix[4]arenes were shown to include a number of other organic guest molecules,^{7–11} among them radicals,^{12–14} allow guest exchange,¹⁵ are capable of forming Langmuir–Blodgett layers,¹⁶ assist topochemical photoreactions,¹⁷ and have proven successfully as adsorbing substance for gases.¹⁸ They have also been studied in view of the structural effects dependent on the length of the acyl chains.^{19,20} Three general types of inclusion structures were found, being additionally controlled by the size and polarity of the guest as well as the crystallization conditions, that is an open container or head-to-tail complex, a nanocapsular or tail-to-tail complex and a partially self-included or interdigitated complex, where the role of the guest is played by another calixarene molecule.¹⁰ Considering the importance of terpenes with regard to their medicinal, cosmetic, odorous and flavouring aspects,²¹ a more profound study of the host behaviour of alkanoyl substituted calix[4]arenes toward the terpenes is worthwhile, for instance concerning their

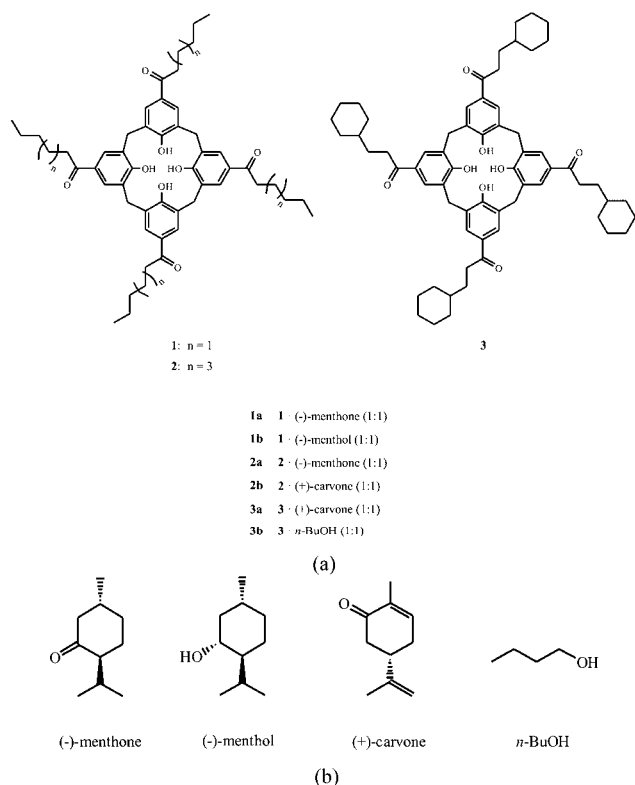
^aInstitut für Organische Chemie, Technische Universität Bergakademie Freiberg, Leipziger Str. 29, D-09596 Freiberg, Sachs., Germany. E-mail: edwin.weber@chemie.tu-freiberg.de; Fax: +49 3731 392386

^bInstitute of Structural Chemistry, Chemical Research Center, Hungarian Academy of Sciences, P. O. Box 17, H-1525 Budapest, Hungary

† This paper is dedicated to Prof. Alajos Kálmán on the occasion of his 75th birthday, who performed prominent work in the fields of isostructurality, morphotropy and polymorphy.

‡ Electronic supplementary information (ESI) available: Additional structural data of the compounds studied by X-ray structural analysis (Tables S1 and S2) and isostructural calculations (Fig. S1–S6). CCDC reference numbers 780763–780768. For ESI and crystallographic data in CIF or other electronic format see DOI: 10.1039/c0ce00696c

§ Present address: University of Oxford, Department of Chemistry, Chemistry Research Laboratory, Mansfield Road, Oxford OX1 3TA, UK.



Scheme 1 Compounds and complexes studied in this paper (a); included guest molecules (b).

protection and storage^{22,23} or chemical sensing using an appropriately modified calixarene.²⁴

Here we report on the synthesis of the upper rim tetraalkanoyl modified calix[4]arenes **1–3** (Scheme 1) of which the 3-cyclohexylpropanoyl substituted derivative **3** is a new compound. Inclusion behaviour of these lipophilically engineered calixarenes towards naturally occurring keto and hydroxylic terpenes as guest molecules is tested, giving rise to the formation of the crystalline complexes **1a**, **1b**, **2a**, **2b** and **3a**, the X-ray crystal structures of which are described and comparatively discussed. In the case of **3**, a solvent inclusion with common *n*-BuOH is also reported, enabling further comparison just as with the previously known inclusion complexes of **1** and **2**. To reveal the extent of isostructurality of the present host frameworks in the solid state influenced by the host substituents and the quality of the guest, isostructurality analysis, cell similarity and molecular isometricity calculations²⁵ were performed. One obvious aim in this respect was to examine how far a crystal structure can tolerate small changes of either host or guest molecules. Moreover, we demonstrate reversible adsorption and desorption properties of the solid calixarenes **1–3** to both vaporous terpene and small solvent molecules using a QMB measurement technique.²⁶

Results and discussion

Synthesis and crystalline inclusion formation

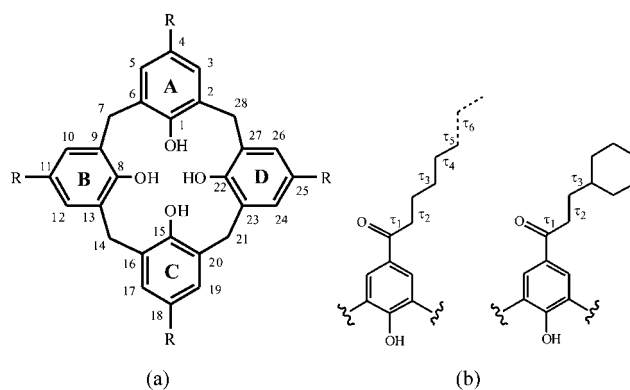
The tetraacyl substituted calix[4]arenes **1–3** (Scheme 1) were prepared in two steps with conventional tetra-*tert*-butylcalix[4]arene as the starting compound.²⁷ These include dealkylation of

the *tert*-butyl groups,²⁸ and a subsequent Friedel–Crafts acylation with the respective acid chloride following a literature procedure.²⁹

Crystallization of **1–3** in solutions of the corresponding guest, or in a mixture with a cosolvent or from a melt of the guest, as specified in the Experimental section, afforded the inclusion compounds **1a**, **1b**, **2a**, **2b**, **3a** and **3b**, respectively (Scheme 1). A number of other potential guest compounds, which were also tested with reference to inclusion formation of the calixarenes **1–3**, proved ineffective. Within the scope of the naturally occurring terpenes, they involve (+)-pulegone, (–)-fenchone and (+)-camphor for all three calixarenes, as well as (+)-carvone for **1**, (–)-menthol for **2**, (–)-menthone and (–)-menthol for **3**. This indicates a distinct selectivity behaviour of the calixarenes. For instance (+)-pulegone, not being included, is close to the monocyclic structures of (–)-menthone or (+)-carvone, while (–)-fenchone and (+)-camphor, also failing in the inclusion, are more bulky bicyclic terpenes.

Crystallographic studies

The inclusion compounds (six species) of the *para*-alkanoyl calix[4]arenes **1–3**, namely **1**·(–)-menthone (1 : 1) (**1a**), **1**·(–)-menthol (1 : 1) (**1b**), **2**·(–)-menthone (1 : 1) (**2a**) and **2**·(+)-carvone (1 : 1) (**2b**), **3**·(+)-carvone (1 : 1) (**3a**), **3**·*n*-BuOH (1 : 1) (**3b**), have been characterized by single-crystal X-ray diffraction. A common atom labelling diagram for the calixarene framework including specification of the arene rings as well as geometrical parameters describing the conformation of the alkanoyl residues are given in Scheme 2. Crystallographic data and selected refinement parameters of the structures are summarized in Table 1. Perspective views of the molecular structures are shown in Fig. 1, 3 and 6 and 7 whereas selected crystal packings are illustrated in Fig. 2, 4, 5 and S1–S6†. In general, the conformation of the calixarene framework (Table 2) can be described by a set of interplanar angles which defines the inclination of the aromatic rings A–D with respect to the reference plane that is given by the methylene atoms C(7), C(14), C(21) and C(28) (Scheme 2(a)). These angles correlate with the dihedral angles between pairs of opposite aromatic rings A/C and B/D, respectively. Corresponding data of



Scheme 2 Labelling diagram of atoms and marking of arene rings of the calixarene core (a); specification of the torsion angles (τ) of the alkanoyl residues (b).

Table 1 Crystallographic and structure refinement data of the compounds studied

Compound	1a	1b	2a	2b	3a	3b
Empirical formula	C ₅₂ H ₆₄ O ₈ ·C ₁₀ H ₁₈ O	C ₅₂ H ₆₄ O ₈ ·C ₁₀ H ₂₀ O	C ₆₀ H ₈₀ O ₈ ·C ₁₀ H ₁₈ O	C ₆₀ H ₈₀ O ₈ ·C ₁₀ H ₁₄ O	C ₆₄ H ₈₀ O ₈ ·C ₁₀ H ₁₄ O	C ₆₄ H ₈₀ O ₈ ·C ₄ H ₁₀ O
Formula weight/g mol ⁻¹	971.28	973.29	1083.48	1079.45	1127.49	1051.40
Crystal system	Monoclinic	Monoclinic	Monoclinic	Monoclinic	Monoclinic	Monoclinic
Space group	<i>P</i> 2 ₁	<i>P</i> 2 ₁ / <i>n</i>				
<i>a</i> /Å	15.7432(3)	15.6344(6)	15.6509(4)	15.6292(3)	15.9123(11)	15.6436(4)
<i>b</i> /Å	22.1360(4)	22.1572(7)	25.0523(6)	23.7075(5)	24.6729(16)	23.5263(5)
<i>c</i> /Å	15.9373(3)	15.8763(5)	15.9443(4)	16.6136(4)	16.1465(10)	15.9163(3)
α /°	90.00	90.00	90.00	90.00	90.00	90.00
β /°	90.294(1)	91.049(2)	90.258(1)	92.02(1)	90.295(4)	91.356(1)
γ /°	90.00	90.00	90.00	90.00	90.00	90.00
<i>V</i> /Å ³	5553.94(18)	5498.9(3)	6251.6(3)	6152.0(2)	6339.1(7)	5856.1(2)
<i>Z</i>	4	4	4	4	4	4
<i>F</i> (000)	2104	2112	2360	2344	2440	2280
<i>D</i> _c /Mg m ⁻³	1.181	1.176	1.151	1.165	1.181	1.192
μ /mm ⁻¹	0.076	0.077	0.074	0.075	0.076	0.077
Data collection						
Temperature/K	133(2)	153(2)	123(2)	103(2)	193(2)	90(2)
No. of collected reflections	100 570	109 553	112 683	108 464	122 207	55 044
Within the θ -limit (°)	1.3–27.4	1.8–26.4	1.3–27.4	1.2–26.3	1.3–25.8	1.5–26.1
Index ranges	–20/20, ± <i>h</i> , ± <i>k</i> , ± <i>l</i>	–19/19, –27/27, –19/18	–18/20, –32/32, –20/19	–19/19, –29/29, –20/20	–16/19, –30/30, –19/19	–10/19, –29/29, –19/19
No. of unique reflections	12 958	11 557	14 540	24 972	12 480	11 587
Refinement calculations: full-matrix least-squares on all <i>F</i> ²						
Weighting expression <i>w</i> ^a						
No. of refined parameters	1342	1329	1446	1479	1506	700
No. of <i>F</i> values used [<i>I</i> > 2σ(<i>I</i>)]	11 174	7972	10 453	18 102	8208	8651
Final <i>R</i> -indices						
<i>R</i> (=Σ Δ <i>F</i> /Σ <i>F</i> _o)	0.0555	0.0524	0.0433	0.0862	0.0710	0.0527
<i>wR</i> on <i>F</i> ²	0.1542	0.1500	0.1126	0.2346	0.2093	0.1402
<i>S</i> (=goodness of fit on <i>F</i> ²)	1.057	1.015	1.040	1.043	1.065	1.065
Final Δρ _{max} /Δρ _{min} /e Å ⁻³	0.54/–0.33	0.55/–0.34	0.35/–0.28	0.55/–0.57	0.50/–0.32	0.55/–0.44

$$^a P = (F_o^2 + 2F_c^2)/3.$$

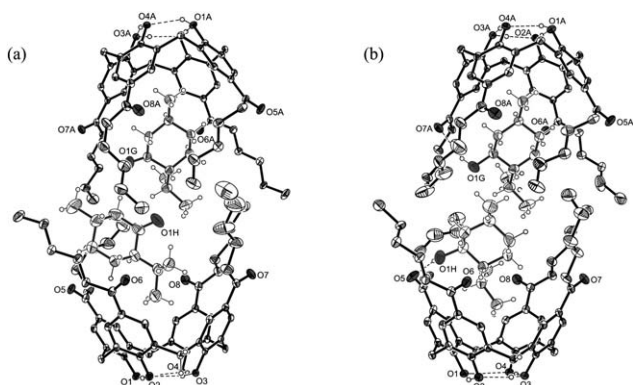


Fig. 1 Perspective views of the asymmetric units of (a) the complex 1·(-)-menthone (2:2) (**1a**) and (b) the 1·(-)-menthol complex (2:2) (**1b**). Thermal ellipsoids are drawn at 40% probability level. For clarity only one position of the disordered parts of the alkanoyl fragments is shown. Broken lines represent hydrogen bonds.

geometric parameters describing the conformation of the alkanoyl branches are summarized in Table S1†. Information regarding hydrogen bond geometries is listed in Table S2†.

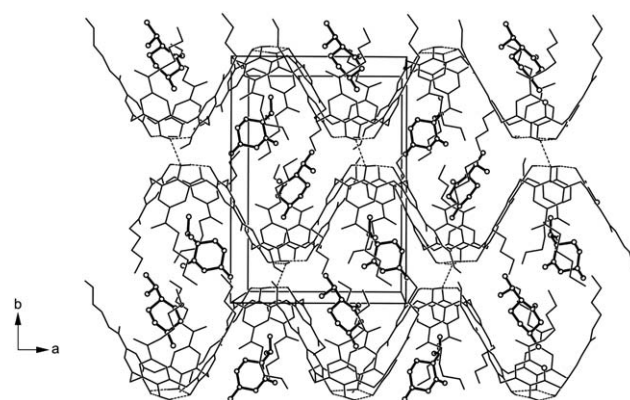


Fig. 2 Packing diagram of the 2:2 complex 1·(-)-menthone (**1a**) viewed down the crystallographic *c*-axis. Calixarene molecules are displayed as wire model, menthone molecules as ball and stick model. Broken lines represent hydrogen bonds.

Results of the isostructurality study are specified in Tables 3 and 4, and illustrated in Fig. S1–S6†.

In the present crystal structures, the calixarene skeleton itself is perfectly ordered whereas the upper rim substituents show higher

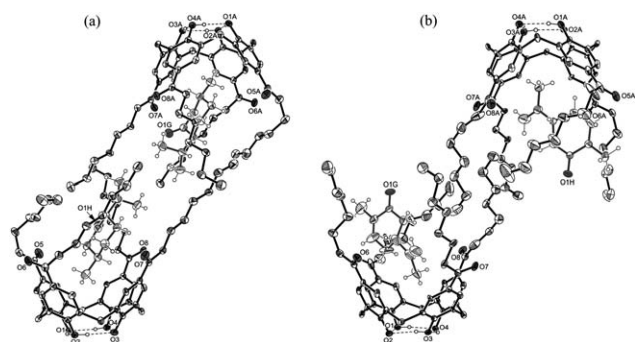


Fig. 3 Perspective views of the asymmetric unit of (a) the complex 2·(-)-menthone (2 : 2) (**2a**) and (b) 2·(+)-carvone (2 : 2) (**2b**). Thermal ellipsoids are drawn at 40% probability level. For clarity only one position of the disordered parts of the alkanoyl fragments is shown. Broken lines represent hydrogen bonds.

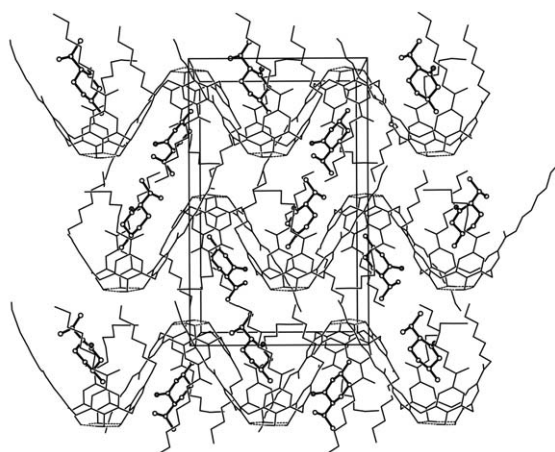


Fig. 4 Packing diagram of the 2 : 2 complex 2·(-)-menthone (**2a**) viewed down the crystallographic *c*-axis. Calixarene molecules are displayed as wire model, menthone molecules as ball and stick model. Broken lines represent hydrogen bonds.

displacement parameters or their terminal carbon atoms are disordered over two positions even at low temperatures. Considering the isostructurality investigation, the atoms with the higher site occupation factor were selected for the respective calculations. For the calixarene–terpene complexes the statistical analysis of *E*-values indicates crystallographic inversion symmetry which, however, is inconsistent with the presence of an enantiomerically pure guest species. A conclusive structure model is represented by the monoclinic space group $P2_1$. This means that the asymmetric entity of the unit cell comprises two crystallographically independent 1 : 1 host–guest complex units. According to the presence of an intramolecular cyclic hydrogen bonding system formed by the phenolic hydroxyl groups, the calixarene molecules are fixed in the cone conformation. The inclusion compounds of the *p*-hexanoyl substituted calix[4]arene **1** with (-)-menthone (**1a**) and (-)-menthol (**1b**) are characterized by nearly identical cell parameters which suggests similarities regarding calixarene geometry and packing behaviour. As shown in Fig. 1, the basic structure elements of **1a** and **1b** consist of pairs of calixarene molecules being arranged in a tail-to-tail fashion to

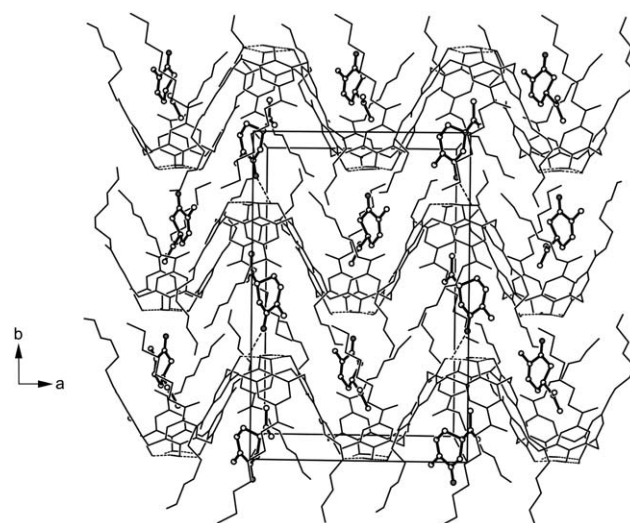


Fig. 5 Packing diagram of the 2 : 2 complex 2·(+)-carvone (**2b**) viewed down the crystallographic *c*-axis. Calixarene molecules are displayed as wire model, carvone molecules as ball and stick model. Broken lines represent hydrogen bonds.

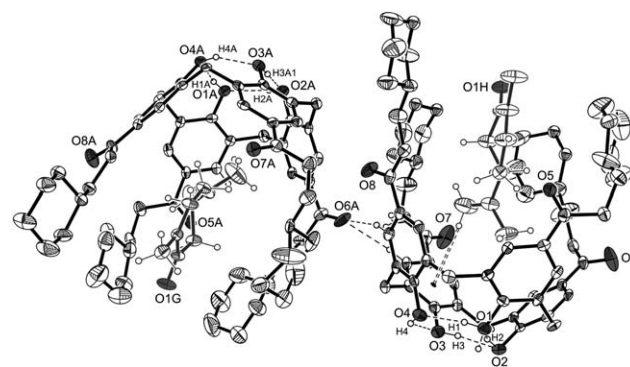


Fig. 6 Perspective view of the asymmetric unit of the complex 3·(+)-carvone (2 : 2) (**3a**). Thermal ellipsoids are drawn at 40% probability level. Broken lines represent hydrogen bonds.

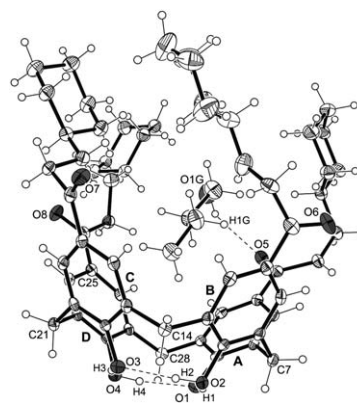


Fig. 7 Perspective view of the complex 3·*n*-BuOH (1 : 1) (**3b**). Thermal ellipsoids are drawn at 40% probability level. Broken lines represent hydrogen bonds.

Table 2 Selected conformational parameters of the cone frameworks

Compound	1a	1a(')	1b	1b(')	2a	2a(')	2b	2b(')	3a	3a(')	3b
Interplanar angles ^{a/f}											
mpla ^b /A	55.7(1)	57.8(1)	59.7(1)	59.2(1)	60.5(1)	60.0(1)	49.5(1)	50.1(1)	50.8(1)	52.6(1)	55.1(1)
mpla/B	57.0(1)	57.2(1)	57.2(1)	56.0(1)	58.0(1)	58.3(1)	61.3(1)	60.2(1)	61.6(1)	59.7(1)	62.1(1)
mpla/C	56.9(1)	54.9(1)	58.3(1)	57.3(1)	58.1(1)	58.2(1)	49.4(1)	50.1(1)	54.4(1)	52.3(1)	56.2(1)
mpla/D	59.9(1)	60.5(1)	58.7(1)	59.9(1)	54.1(1)	54.1(1)	61.9(1)	62.5(1)	57.0(1)	59.8(1)	59.2(1)
A/C	67.5(1)	67.4(1)	62.0(1)	63.5(1)	61.4(1)	61.8(1)	81.1(1)	79.8(1)	74.8(1)	75.1(1)	68.7(1)
B/D	63.1(1)	62.3(1)	64.1(1)	64.1(1)	67.9(1)	67.6(1)	56.8(1)	57.3(1)	61.4(1)	60.5(1)	58.7(1)
mpla ^c /guest ^d	80.0(1)	58.2(1)	50.2(1)	57.3(1)	64.3(1)	63.6(1)	83.4(2)	77.4(2)	82.8(2)	74.1(2)	

^a Aromatic rings: ring A: C(1)⋯C(6); ring B: C(8)⋯C(13); ring C: C(15)⋯C(20); ring D: C(22)⋯C(27). ^b Best plane through atoms C(7), C(14), C(21) and C(28). ^c For (–)-molecules: best plane through atoms C(7A), C(14A), C(21A) and C(28A). ^d Mean plane through the six-membered ring of the terpene guest.

Table 3 Cell similarity indices (π) calculated for **1a–3b**

	1b	2a	2b	3a	3b
1a	0.00674	0.05022	0.02926	0.05144	0.01774
1b	—	0.05658	0.03577	0.05779	0.02432
2a	—	—	0.02206	0.00129	0.03306
2b	—	—	—	0.02338	0.01173
3a	—	—	—	—	0.03552

form molecular capsules. A structural feature worth mentioning is the asymmetric arrangement of the guest molecules within the cavity of the calixarene dimer. In one of the 1 : 1 complex units, the isopropyl residue of the terpene is included into the aromatic cavity of the calixarene whereas in the second complex unit the methyl group is the included residue. Similar structural features are also found in the related (+)-carvone complex of **1**.⁷ Within the capsular complex, the guest molecules are aligned in a head-to-tail mode along the crystallographic *b* axis, showing different degrees of inclination with respect to the reference plane of the calixarene.

Unlike complex **1a**, which lacks directed non-covalent host–guest interactions and thus seems to be primarily stabilized by van der Waals forces, the donor–acceptor nature of the menthol molecules in **1b** allows host–guest binding via O–H⋯O [$d(\text{O}⋯\text{O})$ 3.138(4), 3.187(4) Å] and C–H⋯O [$d(\text{C}⋯\text{O})$ 3.371(4) Å] hydrogen bonds.³⁰ However, maximum saturation of hydrogen bond formation is fulfilled only by one of the menthol molecules whereas in the second one only the hydroxyl hydrogen takes part

in hydrogen bonding. Irrespective of some differences regarding the conformation of the alkanoyl substituents, the packing mode of the calixarene molecules in **1a** (Fig. 2) and **1b** is nearly identical, which will be discussed in detail in the Isostructurality studies section. The crystal structures are both stabilized by a close network of intermolecular interactions with the carbonyl oxygen atoms acting as acceptor sites for ordinary and bifurcated C–H⋯O hydrogen bonds [$d(\text{C}⋯\text{O})$ 3.239(4)–3.568(4) Å (**1a**), 3.314(4)–3.501(5) Å (**1b**)].

In order to elucidate in which way an increase of the alkanoyl chain length influences solid-state structures in general, we were able to determine the crystal structures of **2a** and **2b** obtained from the octanoyl substituted calixarene **2** with (–)-menthone and (+)-carvone, respectively. In each of the 1 : 1 host–guest entities of **2a**, the methyl group of the terpene molecule is located near the aromatic core of the calixarene whereas its isopropyl part is directed out of the cavity (Fig. 3(a)). The host–guest complex is stabilized by C–H⋯ π (arene) contacts³¹ and relatively strong C–H⋯O hydrogen bonds³⁰ (3.087(6), 2.587(5) Å) with the carbonyl oxygens O(1G) and O(1H) acting as acceptors. Also in the complex structure of **2b**, which is depicted in (Fig. 3(b)) the asymmetric unit comprises two non-equivalent 1 : 1 host–guest complexes, which are similar in terms of the molecular conformation.

In both inclusion compounds of **2**, the calixarene molecules are packed in a columnar fashion along the *b* axis accompanied by an elongation of the cell in this direction compared to the complexes of **1** (Table 1). In contrast to the menthone inclusion

Table 4 Molecular isometricity values $I(m)$ (%)

Same host, different guests			Same guest, different hosts		
Compared compounds	Number of atoms fitted	$I(m)$ (%)	Compared compounds	Number of atoms fitted	$I(m)$ (%)
1a(1)–1a(2)	60	63.17	1a(1)–2a(1)	60	53.24
1b(1)–1b(2)	60	27.48	1a(1)–2a(2)	60	16.59
1a(1)–1b(1)	60	24.68	1a(2)–2a(1)	60	77.54
1a(2)–1b(2)	60	72.13	1a(2)–2a(2)	60	40.37
2a(1)–2a(2)	68	21.93	2b(1)–3a(1)	48	63.93
2b(1)–2b(2)	68	48.99	2b(2)–3a(1)	48	70.60
2a(1)–2b(1)	68	21.50	2b(1)–3a(2)	48	69.53
2a(2)–2b(2)	68	19.54	2b(2)–3a(2)	48	63.42
3a(1)–3a(2)	72	68.97			
3a(1)–3b(1)	72	82.78			
3a(2)–3b	72	60.40			

2a, adopting the classical head-to-tail mode (Fig. 4), the respective carvone including structure **2b** shows a closer packing of calixarene molecules because of interpenetrated branches of the long octanoyl residues—probably due to the unsaturated character of carvone with its lack in four hydrogen atoms in comparison to menthone and adopting a more planar geometry (Fig. 5).

In **2b**, two alkyl chains of each calixarene molecule are inserted into the cavities of calixarene molecules of adjacent columns, so that the complex **2b** can be considered as being self-included—the interdigitation of calixarene molecules in **2b** hardly affects the location of guest molecules within the calixarene cavity and the mode of host–guest interaction.

The structure of the host–guest complex of the *p*-(3-cyclohexylpropanoyl) substituted calix[4]arene **3** with (+)-carvone (**3a**) (Fig. 6) resembles those of **1a** and **1b**. However, an appreciable difference is given by the way the carvone molecules are accommodated inside the calixarene cavity. In both 1 : 1 complex units of **3a**, the carbonyl group of the guest molecule points out of the calixarene cavity, so that the complex is stabilized by weak C–H⋯π(arene) contacts³¹ formed between the isopropenyl part of the carvone molecules and aromatic rings A and C (C–H⋯centroid 2.80–2.92 Å). These findings remarkably differ from the crystal structure of the related 1·(+)-carvone complex described in a previous report⁷ which is composed of capsular calixarene dimers with a unique orientation of the included guests.

Thus, modification of the alkanoyl substituents as in **3a** induces significant changes in the complex structure and prevents formation of molecular capsules. Similar to the menthone inclusion **2a**, the crystal structure of **3a** is characterized by a columnar packing of the calixarene complexes in the head-to-tail mode along the *b*-axis (Fig. S5†). The equidistance of the guest oxygens O(1G) and O(1H) to the phenolic oxygens of the neighbouring calixarene molecule [$d(\text{O}\cdots\text{O})$ 2.987(6)–3.010(6) Å] suggests that the hydroxyl hydrogens participate in host–guest binding. Interestingly, although the complexes **2b** and **3a** both contain (+)-carvone as the guest molecule, their packing structures reveal different modes of interaction between the hydrophobic alkyl residues.

Using *n*-BuOH as a solvent, the calixarene **3** yields as colourless crystalline blocks crystallizing in the monoclinic space group $P2_1/n$ with the asymmetric unit containing one host–guest complex of **3b**, the structure of which is displayed in Fig. 7. In the complex **3b**, the calixarene adopts a highly unsymmetrical geometry with one alkanoyl residue being in a fully extended conformation (torsion angles τ_1 – τ_3 *anti*) whereas other two are considerably distorted around their acyl function (torsion angle τ_1 *gauche*). The alcohol molecule is coordinated to one of the carbonyl oxygens by a weak conventional hydrogen bond [O(1G)–H(1G)⋯O(5) 2.36 Å, 141.4°].

Host–guest aggregates in a 2 : 2 ratio with the calixarenes being arranged in a tail-to-tail fashion represent the basic structure motif of the crystal. In the capsular structure of **3b**, the calixarene molecules are shifted such that the cyclohexyl part of one of their alkanoyl branches is located above that of the respective opposite calixarene molecule thus creating a nearly closed calixarene cavity. The packing structure of **3b** is stabilized by a variety of intermolecular C–H⋯O=C hydrogen bonds of different strengths [$d(\text{H}\cdots\text{O})$ 2.29–2.60 Å] and is similar to the

inclusion structures of compound **1** with respect to the tail-to-tail assembly mode (Fig. S6†).

Isostructurality studies

In principle, the crystal structures of the present inclusion compounds exhibit pronounced similarities, but also distinct differences. All synthesized inclusion crystals have similar unit cell dimensions (Table 1) and the cell similarity indices (π)³² are low indicating a high level of metric correspondence (Table 3). Although the crystallographic host : guest stoichiometry 2 : 2 and the space group $P2_1$ are identical for **1a**, **1b**, **2a**, **2b** and **3a** even so only some of them are homostructural, *e.g.* isostructural concerning the host framework. The main difference in the packing arrangements (Fig. S1–S6†) is that the two crystallographically independent calixarene molecules in the asymmetric unit can be found in the same (**1a** and **1b**) or in different (**2a**, **2b** and **3a**) twofold screw axes. In the first case, the head-to-head arrangement forms capsular dimers, the crystallographically independent host molecules are alternating along the crystallographic *b*-axis. In the second case, along the crystallographic *b*-axis head-to-tail columnar arrangement is realized: one column consists of one of the crystallographically independent molecules only.

Furthermore, molecular isometricity [$I(m)$] calculations²⁵ were performed in order to examine the effect of the change in the host substituents and the nature of the guest molecules (Table 4). The molecular geometry of the two crystallographically independent calixarene molecules in the respective asymmetric unit changes less in **1a** and **3a** compared to all the others. As expected, the largest difference occurs in the case of the *n*-octanoyl host substitution—the longer alkyl chain has more freedom of motion. In contrast, the chalice in the 3-cyclohexylpropanoyl substituted compound is the most rigid one among the three types of hosts. Its molecular geometry changes the least with the change of the inclusion guest molecule. Comparing the molecular geometry of the (–)-menthone inclusion complexes **1a** and **2a**, there is a considerable difference in the host conformation in spite of the relatively small difference in the length of the *n*-hexanoyl or *n*-octanoyl substituents. The molecular geometry of the host is more similar compared to *n*-octanoyl and 3-cyclohexylpropanoyl substitution in the (+)-carvone inclusion complexes (**2b** and **3a**, respectively) which is also reflected in the packing arrangement.

At first sight, the packing arrangements of the host molecules in **1a** and **1b** look rather similar. However, there is

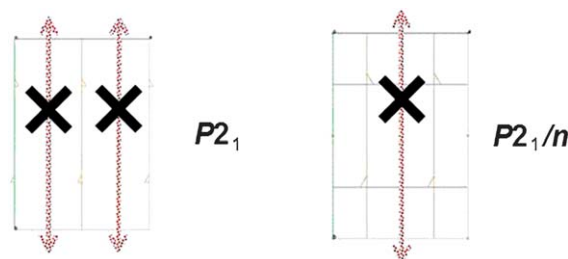


Fig. 8 The space groups $P2_1$ and $P2_1/n$, respectively, viewed along the crystallographic *c*-axis indicating the existing symmetry elements and the virtual twofold axes which organize the morphotropic relation between the morphotropic pairs.

a substantial change in the placement of the molecules in the unit cell thus in packing relations demonstrated by the presentations of the cells from the crystallographic *c*-axis (Fig. S1 and S2†): every second layer is slightly moved to $-a$ (**1a**) or $+a$ (**1b**) direction. The two structures cannot be transformed to each other by crystallographic symmetries determined by the space group without an enantiomeric change. Structure **1a** could be transferred to the arrangement of **1b**, if the two molecules in the asymmetric unit were rotated by a virtual twofold axes parallel to *b* in *a* and *c* at $\frac{1}{4}$ and $\frac{3}{4}$ (Fig. 8). However, there is no twofold axis in the space group $P2_1$. Thus, the host positions in **1a** and **1b** complexes are related by a pseudo-twofold axis, *i.e.* the host frameworks have a morphotropic relation to each other.^{33,34}

Enhancing the supramolecular aspects of polymorphy, the present pair of (–)-menthone and (–)-menthol inclusions of the *n*-hexanoyl substituted calix[4]arene is the second reported example of supramolecular morphotropism. The first described example was the upper rim dinitro substituted and lower rim ethyl ester annexed calix[4]arene molecule crystallized from selected polar protic and aprotic solvents: acetone, DMF, DMSO and *n*-BuOH as guests.³⁵ All these four inclusion compounds have similar cell parameters and identical space group symmetries ($P2_1/n$). Nevertheless, the inclusion of the protic *n*-BuOH molecule does not only affect the host conformation, but it also leads to a substantial change of the packing relations. The location of the calix[4]arene molecule in the unit cell of the previous *n*-BuOH inclusion compound is related to the host position in all other three complexes by a pseudo-twofold axis in the space group $P2_1/n$ (Fig. 8). Obviously, the mode of guest recognition seems to seriously affect the crystal structures. As in the presently reported series of the inclusion compounds, also the *n*-BuOH inclusion complex **3b** crystallizes in the different space group $P2_1/n$ while all others crystallize in $P2_1$. In other words, some molecular changes (either host, guest or host–guest) can be tolerated by the crystal structure. When the tolerance has reached the limit, packing motifs may still be kept but the motifs are moved related to each other. This morphotropic link can be described by non-crystallographic motions.^{33,34} The non-crystallographic movements are the possible outcome of the requirement of close packing, since rotation or migration of the common motif may transform one specific pattern into another with denser packing.

Organic vapour sorption

In view of a potential use of the present lipophilic calixarenes for vapour sensing of terpenes, the vapour adsorption properties of the solid calixarenes were studied by means of a quartz microbalance device.^{26,36} The results obtained with different terpenes (Fig. 9(a)) were compared with a similar QMB experiment using the common organic solvents, cyclohexane, cyclohexene, acetone,³⁷ dioxane and *n*-butanol, which feature functionalities and sizes comparable to the particular terpenes (Fig. 9(b)). In order to better demonstrate the amount of guest uptake, the maximum frequency change after loading (ΔF_{\max}) was converted to the relative mass increase of the gold sensor following the dependency:

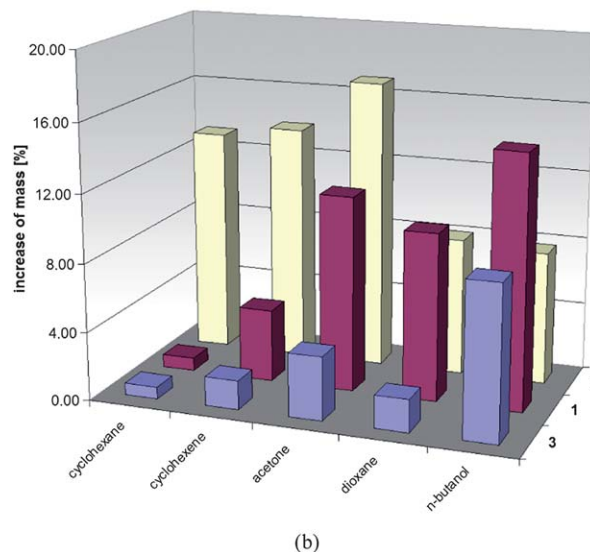
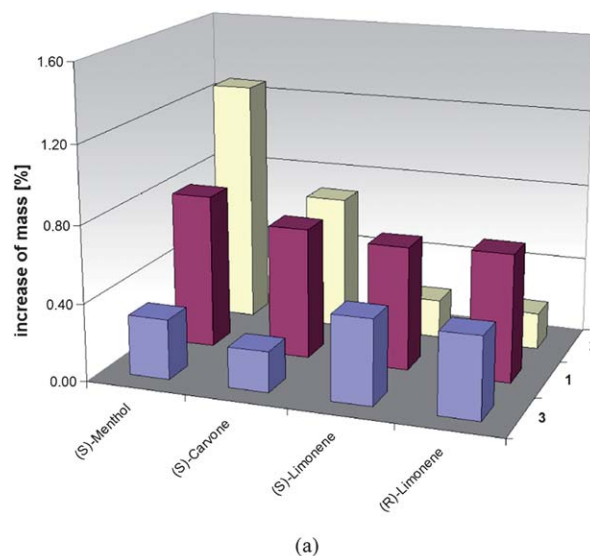


Fig. 9 Relative change of QMB sensor mass for compounds **1–3** against the flow of selected terpenes (a) and solvents (b).

$$\Delta m (\%) = \frac{\Delta F_{\max} - \Delta F_{\text{ref}}}{\Delta F_{\text{ref}}} \times 100\%$$

All experiments involving treatment of the calixarenes with the common solvent vapours show a considerably higher mass increase than for the terpenes. The highest vapour uptake of all was found for the *para*-octanoyl calixarene **2** with acetone (17%). Excepting *n*-butanol, dioxane and limonene (both enantiomers), the total amount of guest uptake is always the largest for the long-chain calixarene **2**. The compound **1** is most efficient in the adsorption of *n*-butanol. On the other hand, the bulky cyclohexyl residues at the upper rim site of the calixarene **3** suggest distinct limitation of the guest uptake with exceptions for *n*-butanol and limonene which are rather equally or even better adsorbed with **3** compared to **2**, respectively. With reference to the polarity of the studied analyte molecules, there is an evident preference of the calixarene **2** featuring long alkyl chains for the adsorption of the apolar hydrocarbons cyclohexane and cyclohexene while

Table 5 Binding stoichiometry (*S*) and host affinity (*a_h*) of compounds **1–3** with selected terpenes and solvents

	<i>S</i>			<i>a_h</i>		
	1	2	3	1	2	3
(<i>S</i>)-Menthol	0.2	0.3	0.1	0.09	0.21	0.09
(<i>S</i>)-Carvone	0.2	0.2	0.1	0.21	0.20	0.13
(<i>S</i>)-Limonene	0.2	0.1	0.1	0.11	0.12	0.01
(<i>R</i>)-Limonene	0.2	0.1	0.1	0.13	0.15	0.06
Cyclohexane	0.1	1.5	0.1	0.02	0.03	0.09
Cyclohexene	0.4	1.5	0.2	0.06	0.06	0.09
Acetone	1.4	2.2	0.5	0.17	0.08	0.19
Dioxane	1.0	1.2	0.2	0.44	0.40	0.51
<i>n</i> -Butanol	1.7	1.2	1.4	0.11	0.34	0.16

otherwise calixarenes **1** and **3** show a moderately higher affinity towards the vapour molecules with polar functionality.

Including the molar weights of host and guest, the binding stoichiometry can be calculated as follows:

$$S = \left(\frac{\Delta F_{\max}}{\Delta F_{\text{ref}}} \right) \left(\frac{M_{\text{host}}}{M_{\text{guest}}} \right)$$

The calculated *S* values in Table 5 again indicate a limited uptake particularly of the larger terpene molecules in the case of the calixarene **3** featuring the bulky terminal cyclohexyl groups. Corresponding to the increase of mass, the small molecules acetone and *n*-butanol also show the highest binding stoichiometry.

As demonstrated by previous studies,³⁸ depending on size and interaction of the analyte molecules, the regeneration step does not always return the sensor frequency to the starting value. This kind of host affinity [*a_h*] towards the different guest uptakes can be expressed by the ratio $1 - (\Delta F_{\max}/\Delta F_{\text{red}})$, where ΔF_{red} is the reduced frequency change observed after incomplete regeneration³⁸ and ΔF_{\max} the respective value after complete regeneration achieved by purging with saturated CH₂Cl₂ vapour. The calculated *a_h* values are also given in Table 5. Except the dioxane uptake of all calixarenes and the adsorption of carvone and menthol for **1** and **2** as well as the adsorption of *n*-BuOH of compound **2**, the rate of regeneration for all other experiments is greater than 80%, *i.e.* the host affinity for vapours of these molecules is very low. In reverse, this points to a significantly higher binding affinity towards dioxane, carvone and menthol which is in agreement with the obtained inclusion structures **1b** and **2a**. Furthermore, it shows that the calixarene coating is thin and enables fast and reversible guest diffusion.³⁸

Conclusions

The introduction of extended alkanoyl substituents attached to the upper rim of a calix[4]arene framework enlarges the cavity volume and thus enables complex formation with terpenes, but also allows inclusion of smaller functionally related guest species of ketone, alcohol and ether type. In this respect, 1 : 1 host–guest complexes represent the basic molecular entities of the present crystal structures, which can be arranged in a tail-to-tail (capsular) or head-to-tail (columnar) fashion. Unexpectedly, the occurrence of capsular host–guest aggregates is in principle less

dependent on the nature of the involved guest species than on the constitution of the host. The crystal structures of the hexanoyl–calixarene inclusion compounds with the ketone (–)-menthone and the alcohol (–)-menthol, **1a** and **1b**, as well as the earlier published (+)-carvone inclusion,⁷ reveal slight deviations of the capsular structure which, however, hardly influence the packing modes. On the other hand, the arrangement of the 1 : 1 host : guest complexes seems indeed affected by the structure and length of the alkanoyl branches: in both inclusion compounds of the octanoyl substituted host **2**, one containing menthone and the other carvone, the calixarene molecules are packed in a columnar fashion along the *b*-axis, which is also true for the carvone inclusion of **3** (**3a**) with even more bulky upper rim substituents. A remarkable structural feature is given in the inclusion structure of **3** with *n*-BuOH (**3b**), in which the small guest component occupies only a part of the calixarene cavity, with the cantilevered in parts cyclic alkyl groups strongly bent towards the calixarene axis in order to reduce the cavity volume. Moreover, the calixarenes comprising the molecular capsule are displaced such that one of their terminal cyclohexyl fragments caps the cavity of the respective opposite calixarene. Both these features could explain the preference of capsular dimers despite the presence of the particularly large upper rim substituents. As shown by this study, calixarenes, bearing hexanoyl groups at the upper rim, prefer the formation of dimeric capsules but octanoyl and longer substituents seem to favor a columnar packing behaviour, which is only valid for the inclusion of guests which fill the entire host cavity. Of special interest for future work in this respect could be the examination of calixarenes substituted with unsaturated (*e.g.* ω-alkenoyl, cyclo-hexenylpropanoyl) residues.

An important aspect in the studies of supramolecular aggregation is the observation that crystal forces alone are often sufficient to influence intramolecular torsion angles of flexible molecules. As an approach to understand the interactions within crystals, calixarenes as semirigid molecules offer ideal conditions to deal with a more limited number of independent variables such as non-crystallographic rotations or translations. In general, a crystal structure is able to tolerate a certain degree of molecular changes and even when the extent of tolerance is reached, common packing motifs may still be kept, although moved, but nevertheless related, to each other. Such a morphotropic link could be shown for the (–)-menthone (**1a**) and (–)-menthol (**1b**) inclusion of the *n*-hexanoyl substituted calixarene (**1**): the change of the guest molecule is inducing a different packing arrangement and thus, this particular case is a rare example of a guest induced supramolecular morphotropism.²⁵

Due to their extended and flexible alkanoyl chains, host compounds **1** and **2** exhibit in some degree disorder in the solid state, but allow on the other hand a moderate inclusion of terpene and solvent vapours. Regarding the cyclohexyl equipped calixarene **3**, the discoidal upper rim residues more or less hinder an effective vapour uptake but develop no noteworthy disorder and so provide a formidable platform for future investigation on the inclusion of lipophilic compounds. QMB measurements demonstrate the predominantly reversible inclusion of both small solvent molecules and terpenes, which is the highest for the calixarene **2** possessing the long and flexible *n*-octanoyl chains. Polar guest molecules and especially those with donor

functionalities show moderately higher host affinities and are exchanged using a special procedure, whereas thin layers of calixarene inclusions with low polar molecules are regenerated in an easy and fast way by purging with air. Following this specific reversible guest binding, all examined *para*-acylcalix[4]arenes potentially establish a new platform for vapour sensing as well as fragrance storage.

Experimental

Melting points were determined on a microscope heating stage PHMK Rapido (VEB Dresden Analytik) and are uncorrected. IR spectra were measured on a Nicolet FT-IR 510 as KBr pellets. NMR spectra were recorded on a Bruker Avance DPX 400 spectrometer at 400 MHz (^1H NMR) and 100.6 MHz (^{13}C NMR), respectively, in CDCl_3 solution. Chemical shifts δ are reported in ppm relative to the internal reference TMS. Elemental analyses were performed on a Heraeus CHN-Rapid Analyzer. The starting compounds 5,11,17,23-tetra-*tert*-butyl-25,26,27,28-tetrahydroxycalix[4]arene and 25,26,27,28-tetrahydroxycalix[4]arene were prepared according to the literature.^{27,28}

Synthesis of host compounds 1–3: general procedure

A mixture composed of aluminium trichloride (118.0 mmol), the respective acid chloride (91.8 mmol) and nitrobenzene (140 cm^3) under an atmosphere of argon was stirred for about 15 min until dissolution. 25,26,27,28-Tetrahydroxycalix[4]arene (15.3 mmol) was added, the solution stirred for 4 h, then poured onto ice and kept for 1 h. The organic phase was separated and the aqueous phase extracted twice with chloroform (250 cm^3). The combined organic phases were washed with 1 M hydrochloric acid (2 \times 270 mL), a mixture of 1 M brine and 1 M aqueous sodium acetate, and water (2 \times 250 cm^3 , each time) in this sequence. The chloroform was evaporated under reduced pressure and the nitrobenzene removed by steam distillation. Recrystallization from acetone/chloroform (1 : 1) yielded the pure products. Specific details of the compounds are given below. For calixarenes **1** and **2** we were unable to reproduce the melting points reported in the literature,²⁹ which we explain with the behaviour of polymorphism occurring in this particular class of calixarenes.³⁹

5,11,17,23-*p*-Tetrahexanoyl-25,26,27,28-tetrahydroxycalix[4]arene (1). Yield 47%; mp 165–166 °C (lit.,²⁹ 183 °C). The other analytical data correspond with the literature.

5,11,17,23-*p*-Tetraoctanoyl-25,26,27,28-tetrahydroxycalix[4]arene (2). Yield 53%; mp 177–178 °C (lit.,²⁹ 145 °C). The other analytical data correspond with the literature.

5,11,17,23-*p*-Tetrakis(3'-cyclohexylpropanoyl)-25,26,27,28-tetrahydroxycalix[4]arene (3). Yield 86%; mp 167–169 °C; IR (KBr) 3229, 3043, 2924, 2852, 1683, 1600, 1445, 1326, 1316, 1284, 1166, 788; ^1H NMR (CDCl_3) 0.88, 1.23, 1.55, 1.67 (4 m, 48H, AlkylH), 2.18 (s, 4H, CH), 2.84 (t, 8H, COCH₂), 3.73 (s, br, 4H, ArCH₂Ar), 4.28 (s, br, 4H, ArCH₂Ar), 7.76 (s, 8H, ArH), 10.20 (s, 4H, OH); ^{13}C NMR (CDCl_3) 26.2, 26.5, 31.7, 31.9, 33.2, 35.8, 37.3 (AlkylC), 127.7, 129.8, 132.00 (ArC), 152.6 (ArC–OH),

198.7 (C=O). Anal. calcd for $\text{C}_{64}\text{H}_{80}\text{O}_8$: C, 78.65; H, 8.25; found: C, 78.40; H, 8.24%.

Vapour sorption experiments

The experimental setup of the quartz crystal microbalance consists of two 10 MHz standard electronic quartzes with gold electrodes (FOQ Piezo Technik, Germany). One of them is uncoated and used as a reference; the other one is coated with the receptor (solid calixarene). Both quartzes are located in a thermostatted metal block (controlled to 25 °C by a water thermostat). The measurements are carried out with a constant flow of synthetic air. The resonance frequencies of the quartzes are measured by a multichannel frequency counter (HKR sensor systems Munich, Germany) with a resolution of 1 Hz. The frequency data can be read by the computer *via* a serial interface. The coating of the quartzes was performed by dipping the quartz for 30 s in a 0.1 molar solution of the respective calixarene in methylene chloride and afterwards drying *via* air stream for 30 min. This coating gives a constant decrease of the oscillator frequency of about ~2200 Hz, which was chosen as ΔF_{ref} . Together with the Sauerbrey-constant S_f of the quartz crystal ($0.12 \pm 0.02 \text{ Hz cm}^2 \text{ ng}^{-1}$, 10 MHz, TSM, polished gold electrodes) and the mean density of the calixarene inclusions (ρ_{cal}), calculated from the X-ray data, the average thickness of the host layer (d_a) was estimated to be ~150 nm using the equation:

$$d_a (\text{nm}) = \frac{\Delta F_{\text{ref}} \times 10^{-2}}{S_f \times \rho_{\text{cal}}}$$

According to the literature,³⁸ such a thin film meets the demands regarding fast diffusion and reversibility of the binding event. In a typical QMC sensor experiment, after 300 s equilibration time, the saturated headspace vapour of a guest substance in an upstreamed flask was channeled *via* a constant air stream across the sensor cell for 600 s. After this loading time, a reequilibration time of further 300 s was added to return to the starting frequency. The frequency difference and increase of mass were determined with an error of 5%.

X-Ray diffraction‡

The crystals suitable for X-ray investigations were obtained as follows: crystallization of **1** from a solvent mixture of (–)-menthone/EtOH (9 : 1) and from a melt of (–)-menthol yielded the respective inclusion compounds **1a** and **1b** (Scheme 1). Slow evaporation of a solution of **2** in (–)-menthone/EtOH (9 : 1) solvent mixture afforded suitable crystals of the (–)-menthone inclusion **2a**. The inclusion compounds **2b** and **3a** were obtained *via* crystallization from solutions of **2** and **3** in (+)-carvone. Similarly, **3b** was prepared from **3** and *n*-BuOH as guest solvent.

The intensity data were collected on a Bruker APEX II diffractometer with MoK_α radiation ($\lambda = 0.71073 \text{ \AA}$) using ω - and ϕ -scans. Reflections were corrected for background, Lorentz and polarization effects. Preliminary structure models were derived by application of direct methods⁴⁰ and were refined by full-matrix least squares calculation based on F^2 for all reflections.⁴¹ An empirical absorption correction based on multi-scans was applied by using the SADABS program.⁴² With the

exception of the phenolic hydrogens in **3a** all other hydrogen atoms were included in the models in calculated positions and were refined as constrained to bonding atoms.

Acknowledgements

Financial support from the German Federal Ministry of Economics and Technology (BMWi) under grant No. 16IN0218 'ChemoChips' is gratefully acknowledged. This work was also supported by the Hungarian Research Fund T049712.

References

- C. D. Gutsche, *Calixarenes: an Introduction (Monographs in Supramolecular Chemistry)*, Royal Society of Chemistry, Cambridge, 2008.
- S. J. Dalgarno, P. K. Thallapally, L. J. Barbour and J. L. Atwood, *Chem. Soc. Rev.*, 2007, **36**, 236 (and references therein).
- P. K. Thallapally, B. P. McGrail, S. J. Dalgarno, H. T. Scharf, J. Tian and J. L. Atwood, *Nat. Mater.*, 2008, **7**, 146–245.
- P. K. Thallapally, B. P. McGrail and J. L. Atwood, *Chem. Commun.*, 2007, 1521–1523.
- P. K. Thallapally, B. P. McGrail, S. J. Dalgarno and J. L. Atwood, *Cryst. Growth Des.*, 2008, **8**, 2090–2092.
- W. Sliwa and C. Kozłowski, *Calixarenes and Resorcinarenes*, Wiley-VCH, Weinheim, 2009, pp. 103–180.
- G. Ramon, A. W. Coleman and L. R. Nassimbeni, *Cryst. Growth Des.*, 2006, **6**, 132–136.
- P. Shahgaldian, A. W. Coleman, B. Rather and M. Zaworotko, *J. Inclusion Phenom. Macrocyclic Chem.*, 2005, **52**, 241–245.
- A. Dubes, K. A. Udachin, P. Shahgaldian, A. N. Lazar, A. W. Coleman and J. A. Ripmeester, *New J. Chem.*, 2005, **29**, 1141–1146.
- G. S. Ananchenko, K. A. Udachin, M. Pojarova, A. Dubes, J. A. Ripmeester, S. Jebors and A. W. Coleman, *Cryst. Growth Des.*, 2006, **6**, 2141–2148.
- M. Pojarova, G. S. Ananchenko, K. A. Udachin, M. Daroszewska, F. Perret, A. W. Coleman and J. A. Ripmeester, *Chem. Mater.*, 2006, **18**, 5817–5819.
- G. S. Ananchenko, M. Pojarova, K. A. Udachin, D. M. Leek, A. W. Coleman and J. A. Ripmeester, *Chem. Commun.*, 2006, 386–388.
- G. S. Ananchenko, K. A. Udachin, A. W. Coleman, D. N. Polovyanenko, E. G. Bagryanskaya and J. A. Ripmeester, *Chem. Commun.*, 2008, 223–225.
- D. N. Polovyanenko, E. G. Bagryanskaya, A. Schnegg, K. Möbius, A. W. Coleman, G. S. Ananchenko, K. A. Udachin and J. A. Ripmeester, *Phys. Chem. Chem. Phys.*, 2008, **10**, 5299–5307.
- G. S. Ananchenko, K. A. Udachin, A. Dubes, J. A. Ripmeester, T. Perrier and A. W. Coleman, *Angew. Chem., Int. Ed.*, 2006, **45**, 1585–1588.
- P. Shahgaldian, M. Cesario, P. Goreloff and A. W. Coleman, *Chem. Commun.*, 2002, 326–327.
- G. S. Ananchenko, K. A. Udachin, J. A. Ripmeester, T. Perrier and A. W. Coleman, *Chem.-Eur. J.*, 2006, **12**, 2441–2447.
- G. S. Ananchenko, I. L. Moudrakovski, A. W. Coleman and J. A. Ripmeester, *Angew. Chem., Int. Ed.*, 2008, **47**, 5616–5618.
- M. Pojarova, G. S. Ananchenko, K. A. Udachin, F. Perret, A. W. Coleman and J. A. Ripmeester, *New J. Chem.*, 2007, **31**, 871–878.
- G. S. Ananchenko, K. A. Udachin, M. Pojarova, S. Jebors, A. W. Coleman and J. A. Ripmeester, *Chem. Commun.*, 2007, 707–709.
- E. Breitmaier, *Terpenes. Flavors, Fragrances, Pharmaca, Pheromones*, Wiley-VCH, Weinheim, 2006.
- D. Bockmühl, R. Breves, M. Weide and J. Boy, *PCT Int. Appl.*, 2005, 120, 229.
- M. Weide, D. Bockmühl, T. Gerke, A. Bolte, R. Breves and S. Döring, *PCT Int. Appl.*, 2004, 110, 147.
- T. Gruber, C. Fischer, M. Felsmann, W. Seichter and E. Weber, *Org. Biomol. Chem.*, 2009, **7**, 4904–4917.
- A. Kálmán and L. Párkányi, in *Advances in Molecular Structure Research*, ed. M. Hargittai and I. Hargittai, JAI Press, Greenwich, 1997, vol. 3, pp. 189–226.
- V. I. Kalchenko, I. A. Koshets, E. P. Matas, O. N. Kopylov, A. Solovyov, Z. I. Kazantseva and Y. M. Shirskov, *Mater. Sci.*, 2002, **20**, 73–88.
- C. D. Gutsche, M. Iqbal and D. Stewart, *J. Org. Chem.*, 1986, **51**, 742–745.
- C. D. Gutsche and J. A. Levine, *J. Am. Chem. Soc.*, 1982, **104**, 2652–2653.
- P. Shahgaldian, A. W. Coleman and V. I. Kalchenko, *Tetrahedron Lett.*, 2001, **42**, 577–579.
- G. R. Desiraju and T. Steiner, *The Weak Hydrogen Bond*, Oxford University Press, Oxford, 1999.
- M. Nishio, *CrystEngComm*, 2004, **6**, 130–158.
- A. Kálmán, L. Párkányi and G. Argay, *Acta Crystallogr., Sect. B: Struct. Sci.*, 1993, **49**, 1039–1049.
- A. Kálmán, *Acta Crystallogr., Sect. B: Struct. Sci.*, 2005, **61**, 536–547.
- A. Kálmán and L. Fábrián, *Acta Crystallogr., Sect. B: Struct. Sci.*, 2007, **63**, 411–417.
- T. Gruber, E. Weber, W. Seichter, P. Bombicz and I. Csöreg, *Supramol. Chem.*, 2006, **18**, 537–547.
- U. Schramm, C. E. O. Roesky, S. Winter, T. Rechenbach, P. Boeker, P. Schulze Lammers, E. Weber and J. Bargon, *Sens. Actuators, B*, 1999, **57**, 233–237.
- We also succeeded in obtaining a 1 : 1 inclusion of calixarene **3** with acetone from a mixture of acetone-chloroform (1 : 1). In this special case the host molecules are arranged in a tail-to-tail fashion similar to compound **3b**. Unfortunately, because of the low quality of the crystals we were unable to solve the structure to a sufficiently high level.
- L. S. Yakimova, M. A. Ziganshin, V. A. Sidorov, V. V. Kovalev, E. A. Shokova, V. A. Tafeenko and V. V. Gorbachuk, *J. Phys. Chem. B*, 2008, **112**, 15569–15575.
- S. Shinkai, T. Nagasaki, K. Iwamoto, A. Ikeda, G.-X. He, T. Matsuda and M. Iwamoto, *Bull. Chem. Soc. Jpn.*, 1991, **64**, 381–386.
- G. M. Sheldrick, *SHELXS-97: Program for Crystal Structure Solution*, University of Göttingen, Germany, 1990.
- G. M. Sheldrick, *SHELXL-97: Program for Crystal Structure Refinement*, University of Göttingen, Germany, 1997.
- G. M. Sheldrick, *SADABS*, University of Göttingen, Germany, 2004.